Proceedings of the
International Conference on Mechanical Engineering 2011
(ICME2011) 18-20 December 2011, Dhaka, Bangladesh

ICME11-FL-014

TAPER AND ANGLE OF ATTACK PERFORMANCE COMPARISON FOR UNTWISTED BLADE WIND TURBINE

A.B. Mahmud Hasan, **Ziaul Huque**, **Donald Harby and Raghava Kommalapati**

Center for Energy and Environmental Sustainability (CEES), Prairie View A&M University, USA

ABSTRACT

Numerical simulation of horizontal axis wind turbines (HAWTs) with untwisted but tapered blade was performed to determine the comparison of blades on tapering and angle of attack (AOA) that can produce the highest power output. Numerical solution was carried out by solving conservation equations in a non-rotating reference frame wherein the blades were not in motion. Two different blades on tapering (25% and 50%) are compared for attached flow conditions and the flow physics around the geometries are analyzed. The tapering effect of the profile's original size in the span direction is considered. To this end, the pressure coefficient (C_p) is defined based on the stagnation pressure rather than on the inflow dynamic pressure. Results indicate from the comparison that better tapered shape that produced torque and thrust in both forces and moments is a geometry that has the higher tapering from beginning to end of airfoil profiles along span direction. Numerical experiments were then conducted by varying the angle of attacks of 0^o and 5.8^o. Increasing angle of attack has prominent effect on performance of wind turbine. The work here presented shows that CFD may prove to be useful to complement 2D based methods on the design of new wind turbine blade tapering and angle of attacks.

Keywords: Tapered Blade, Angle of Attacks, Untwisted Blade, Pressure Coefficient, Skin Friction Coefficient.

1. INTRODUCTION

The energy problems we are facing today are articulated around two main drivers: supply and greenhouse gas emissions. Renewable energy sources are an inevitable part of the solution. Wind energy is undoubtedly one of the cleanest forms of power from a renewable source. Wind turbine makes no air pollution as it is not fossil fuels and no burning associated with it. As a new type of renewable energy, wind power is being increasingly used and is currently the fastest growing installed production technology. In order for wind energy to be a viable alternate energy source and compete with fossil fuels, it is extremely important to optimize electricity generation efficiency by determining the optimum shape of the turbine blades, the angle by which free stream wind will hit the blade along with the appropriate materials used to construct the blades.

Wind turbine blade design mainly relies on Blade Element Momentum (BEM) [1] based methods, using optimization techniques to obtain optimal chord and twist distributions along the blade once appropriate airfoils have been chosen. BEM methods are very fast and reliable in the design process, nevertheless these are limited due to their two dimensional nature. These codes require tabulated data for the lift, drag and moment distributions versus the angle of attack to calculate the blade aerodynamic loads. Furthermore, empirical corrections are necessary to account for rotational effects near the root and three dimensional (3D) flows around the tip region, Glauert [2].

Limited research has been published on the use of CFD to design new blade shape for wind turbines. Johansen and Sorensen [3] studied three different tips from the Tellus experiment at different wind speeds and extracted some conclusions on how tapering and swept angle can influence on blade loading. Ferrer, et. al. [4-6] performed studies on three wind turbine blade tip designs with a fixed twist and no tapering at all designs. They have analyzed the complex flow physics using a full Navier-Stokes code. The work showed how CFD can complement BEM methods in the design process. Without considering tapering effect their work leaded to limited capability to use in current market available design of wind turbine blades, where tapering is a must to consider parameter to get better performance of wind turbine.

The angle of attack is another important parameter as analyzed by Thumthae et al. [7]. Their work defined 3D modeling with untwisted blade for different angle of attacks. However, comparison between 0^o and higher

angle of attacks (5.8°) were not made in their analysis. Therefore, analyzing this parameter would be very important when wind flows such a high angle of attacks.

2. RESEARCH OBJECTIVES

Due to importance of lift and thrust in wind turbine, this research is trying to observe behavior of C_p (coefficient of pressure) and C_f (skin friction coefficient) curves due to tapering and angle of attack at first on 2D and later 3D airfoils. The main objective of the current work is to determine the effect of tapering and angle of attack added to the Ferrer's [6] concept of variation of blade profile along span direction. The blade was chosen consists of NERL Phase-VI (which is also known as S809).

As coefficient of pressure, C_p, around an airfoil is closely related to the lift and drag of the wind turbine the analysis of this variable is very important. Absolute pressure has been divided by the stagnation pressure to obtain the retained pressure coefficient as shown in equation 1, instead of using the classical definition for C_p as shown in equation 2.

$$C_p = \frac{(P - P_\infty)}{(P_{stagnation} - P_\infty)} \quad (1)$$

$$C_p = \frac{(P - P_\infty)}{\frac{1}{2}.\rho_\infty.[(\Omega.r)^2 + V_\infty^2]} \quad (2)$$

Where,

Ω	is the rotational speed of the blade
r	is the radius
V_∞	is the wind speed
P_∞	is the free stream pressure
ρ_∞	is the free stream density

The classical definition, equation 2, assumes that for the same section, all tips would see the same free stream dynamic pressure at the stagnation point and does not take into account the local induction factors that are modified by the local blade geometry and rotation. At a given station, the stagnation pressure varies depending on the blade tip shape. The retained definition shows the effective sectional loading, which would not be seen if the classical definition was used. With the retained definition, the C_p area (curve integral) is directly related to the sectional normal force coefficient.

3. METHODOLOGY

Initial CFD simulations of air flow around a 2D wind turbine blade were performed. NREL phase-VI airfoil was used for non-rotating blades without any taper and twist. Two values of free stream velocities of 9 (for tapering) and 8.5 (for angle of attacks) m/s with steady k-ε Realizable turbulent model and no-slip boundary conditions were considered for flow simulation. Other than inlet boundary condition for free stream flow, all other boundary conditions are considered as pressure outlet/outflow (that means constant pressure condition).

At first 2D (two dimensions) simulations have been conducted which consist of structured meshing around airfoil and surrounding computation regions. This gives basic idea of simulating 3D airfoil. However, rather than using structured meshing for 3D we have considered unstructured meshing. Unstructured meshing in 3D gives flexibility to mesh in tiny areas where structured meshing is not possible. Current literatures inform us that 3D wind turbine simulations have been conducted on unstructured meshing [6, 7], however 2D simulations are conducted on structured meshing [8].

For the simulations, chord length (c) of airfoils are considered as 1 m, width of airfoil varies with length, span length of airfoils for 3D are considered as 5m, and all the airfoils are considered as solid material. For fluid properties the pressure values considered as 101325 Pa, density as 1.225 kg/m^3, and kinematic viscosity as 1.4607x10^{-5} m^2/s.

Gambit software is considered for pre-processing that includes drawing, assigning boundary conditions, and meshing the computational domain. After that Fluent which is a finite volume (FV) solver software to post-process the assigned numerical problem is used.

The code from COMSOL was used with 14,559 unstructured mesh elements. Results were obtained for several angle of attacks, α=0 ° and 5.8°.

Figure 1 shows a close up view of meshes around the 2D NREL phase-VI airfoil. This figure indicates the denser meshes around airfoil especially at the leading and trailing edge of the airfoil. Leading edge deals with the effect of stagnation phenomena and trailing edge deals with flow separation from airfoil. Structured elements have been considered for the domain. Figure-1(b) shows zoomed (close up) view of meshes around airfoil.

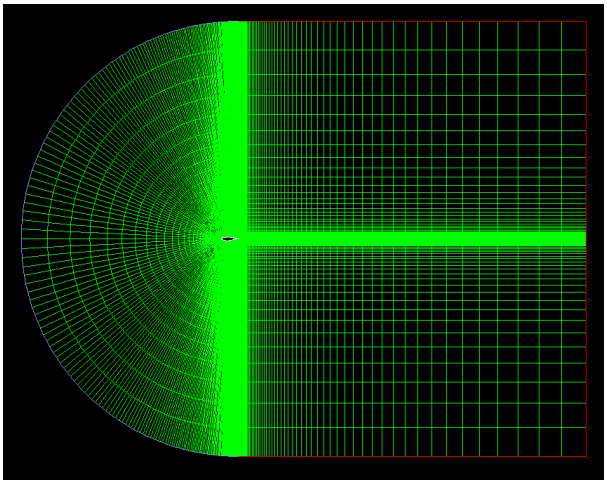

(a)

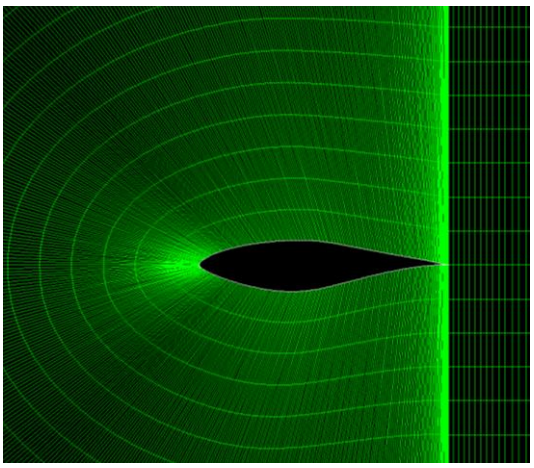

(b)

Fig 1. Meshes in: (a) whole computational domain (b) around airfoil

Figure-2 shows unstructured meshing around 3D NREL Phase-VI airfoil in different views. This 3D meshing represents the 2D meshings to get the effect of variation of taperings in z direction. To draw 3D airfoil the extrusion process has been conducted on 2D airfoil profile with 0% (uniform/no tapering), 25% and 50% tapering along span direction.

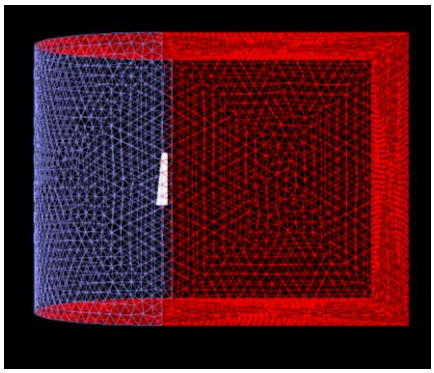

(a)

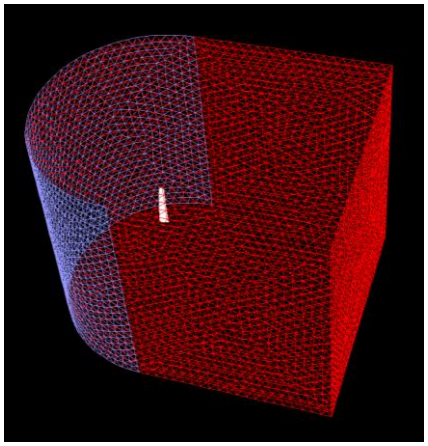

(b)

Fig 2. 3D meshing in 50% tapered airfoil (a) side view (b) isometric view

4. RESULTS AND DISCUSSIONS

Numerical simulations have been conducted for turbulent, untwist, and non-tapered (uniform chord length along span direction) for 2D and 3D as well as varying percentage of tapers (25% and 50%) up to end along span direction for 3D airfoil.

In figure-3 it is found that due to free stream velocity of 9 m/s, flow hits the airfoil and eventually deflects around airfoil periphery. When flow hits the leading edge of airfoil, stagnation of flow occurs which is indicating by blue color in figure-3. However, flow accelerates and get higher velocity values at top and bottom surface of airfoil indicating by red color. There is little variation of velocities at top and bottom surface of airfoil which will have effect on lift of airfoil. Arrow plots for velocity have also been shown in figure-3 (b). No velocity (no slip) has been observed over the surface of airfoil.

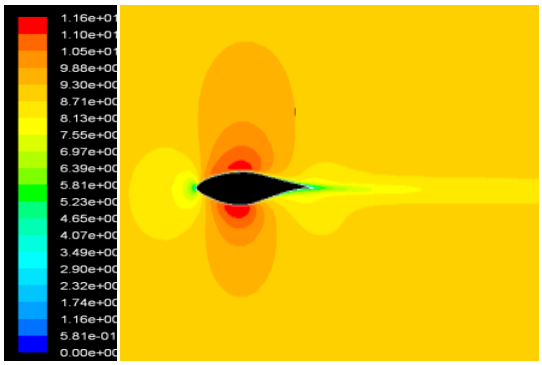

(a)

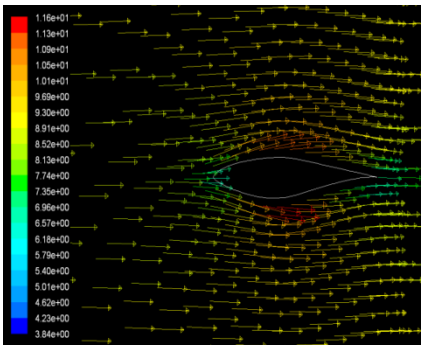

(b)

Fig 3. Velocity (a) contours (b) vector arrows around airfoil for angle of attack (α) =0^o

In figure-4 contour plot of vorticity has been shown. This figure also has close relationship with figure-3 (velocity). Vorticity develops at the trailing edge of airfoil which causes the flow deflected from the airfoil.

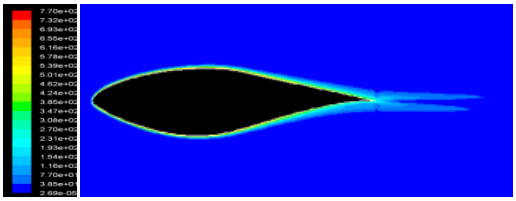

Fig 4. Contour of vorticity magnitude around airfoil for angle of attack (α) =0^o

Pressure profile for this airfoil has been shown in figure-5. The leading, trailing, top and bottom edge of airfoil seems have variation of pressures. Top and bottom side of pressure change is measured and is shown in figure-6 by pressure coefficient values.

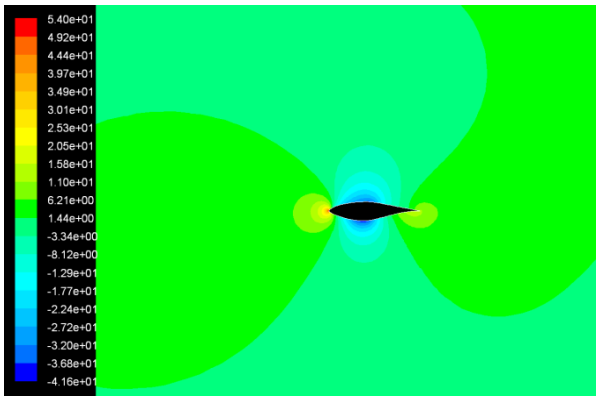

Fig 5. Pressure contours around airfoil for angle of attack (α) =0^o

The top and bottom side coefficient of pressure distributions along chord direction is shown in figure 6. C_p values for bottom side are higher (around 10 times at x/c=0.3) than top side for up to non-dimensionalised chord length. However, after that C_p value for top side is higher (around 10 times at x/c=0.8) than bottom side for up to non-dimensionalised chord length of around 1.0 (end of chord length of airfoil). This variation has proportional relation on lift effect on airfoil.

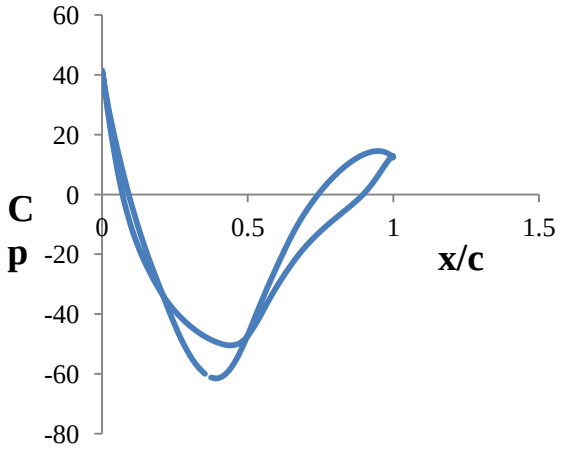

Fig 6. Cp versus x/c curve for 2D airfoil for angle of attack (α) =0^o

Skin friction coefficient (C_f) is a good parameter to find drag effect on airfoil. Skin friction coefficient (C_f) is calculated using the equation:

$$C_f = \frac{\tau_w}{\frac{1}{2}\rho_\alpha U_\alpha^2} \qquad (3)$$

Here, τ_w =Shear stress at wall, ρ_α =Free stream flow density, U_α =Free stream velocity.

Figure-7 and 8 shows skin friction coefficient values around airfoil. Figure 7 shows that there is drag all over the airfoil, however flow gets resistance due to airfoil profile becomes wider on top and bottom surfaces of airfoil at the middle of the chord. In those regions prominent effects of drag have been observed. Figure-8 shows skin friction coefficient effect along chord length.

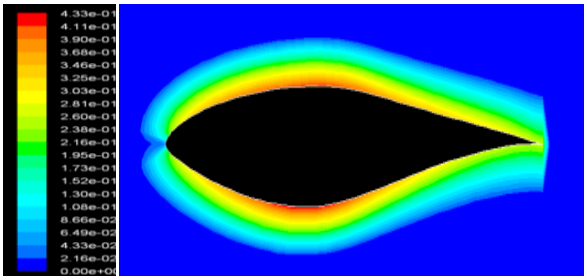

Fig 7. Skin friction coefficient around airfoil for angle of attack (α) =0^o

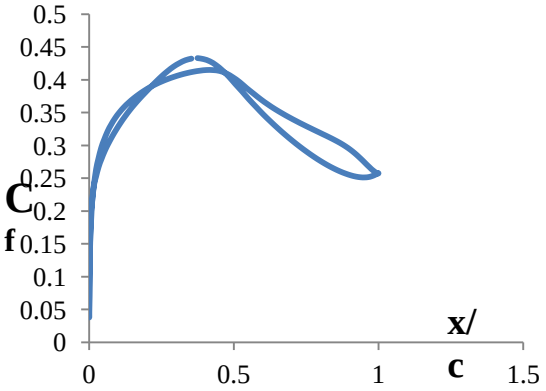

Fig 8. C_f versus x/c curve for 2D airfoil for angle of attack (α) =0^o

From figure 8 it is observed that C_f value is much less (around 150 times at x/c=0.3) than C_p value as observed in figure 6. This kind of lower value is desirable in a wind turbine blade because the higher value of skin friction will lead to reduce the flow around airfoil and eventually increase drag and vice versa.

To validate that the number of meshes for the already run case is the right amount to get the right results, mesh independence test has been conducted with considering higher number of elements than the already run case. The obtained results are shown in figure-9. It seems like the results of the already run case and higher number of elements show very less difference (around 2% at x/c=0.4) in the value of C_p values on top surface of airfoil. This test indicates the number of meshes for the already run case is the right amount and no need to consider higher number of elements which can reduce the speed of computations.

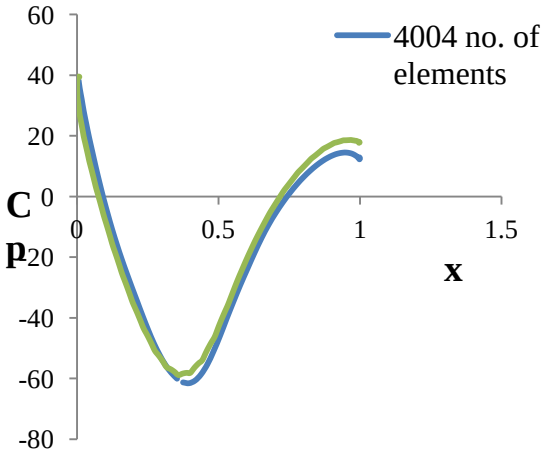

Fig 9. Mesh independence test 2D airfoil top surface for angle of attack (α) =0^o

After that, 3D simulations have been conducted to get the effects of tapering on simulations. After around 70K, 85K, and 130K iterations for 0% (uniform), 25% and 50% tapered blade respectively the velocity and pressure contour plots have been shown in figure-10 and 11. Where, K means 1000. All other necessary parameters e.g. C_p and C_f values have also been shown in later figures based on the above iterations.

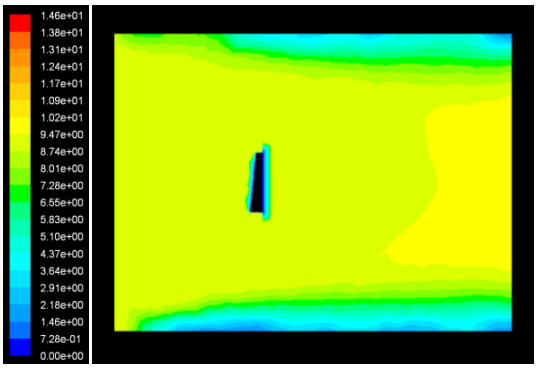

(a)

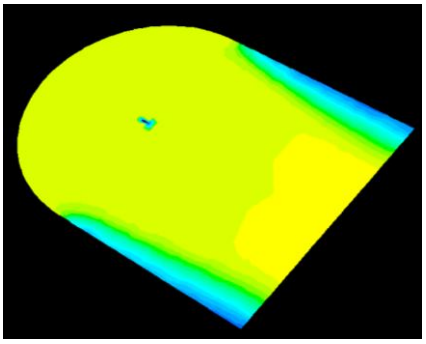

(b)

Fig 10. Velocity magnitude in 50% tapered blade for angle of attack (α) =0^o on cross-sectional plane (a) 50% at chord length (b) 50% at span length

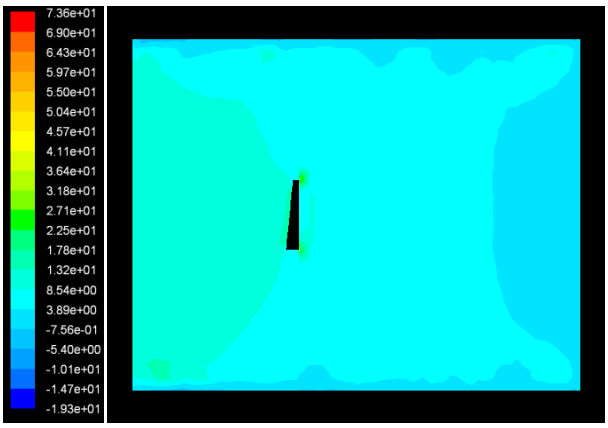

(a)

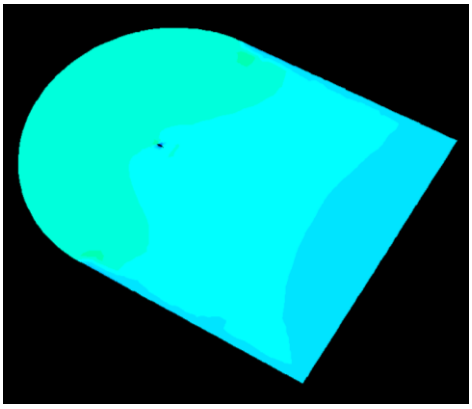

(b)

Fig 11. Pressure values in 50% tapered blade for angle of attack (α) =0^o on cross-sectional plane (a) 50% at chord length (b) 50% at span length

Comparison of C_p values for 0% (uniform) and 50% tapered surface indicates effects of taper on C_p values as shown in figure-12. Uniform blade and 50% tapered blade have little variation (less than 1% at x/c=0.8) on the bottom surface of airfoil, however separate simulations (not shown in the figure) for 25% tapered blade indicates higher C_p values (around 50% difference at x/c=0.7) at top surface of airfoil other than the values at the middle of chord length. As top surface needs to have lower pressure and bottom surface needs to have higher pressure to get better lift, therefore 25% tapered airfoil which gives higher C_p values on the top side of airfoil surface might not be a good design.

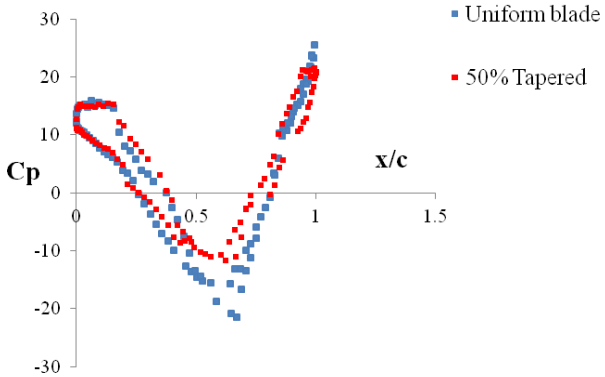

Fig 12. Tapering effect on C_p versus x/c curve for angle of attack (α) =0^o

Comparison of C_f values for uniform and 50% tapered surface indicates effects of taper on the top and bottom sides of airfoil as shown in figure-13. C_f value indicates the drag value due to friction between fluid and surface of airfoil. Higher of this value will not lead to performance enhancement of wind turbine. At 50% tapered blade the C_f values decrease (around 2% at x/c=0.3) along chord length of airfoil. However, separate simulations on 25% tapering of the blade indicates increased C_f values (around 1.7 times at x/c=0.3). This validates the findings made by Ferrer et al. [6] that blade tip needs to be tapered high enough (25% might be less and 50% might be reasonably tapered) to improve the blade performance. The results also indicated that if tapering is not considered high enough the blade performance will decrease.

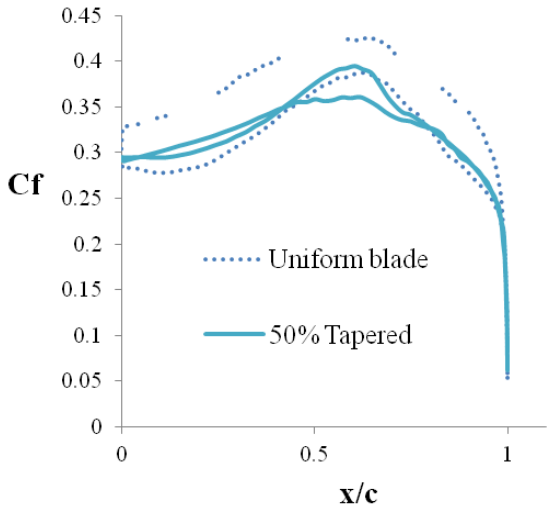

Fig 13. Tapering effect on C_f versus x/c curve for angle of attack (α) =0^o

After that, variation of angle of attacks for flow passes over airfoil has been analyzed using Comsol software. Comsol (previously known as Femlab) is a finite element (FE) software that helps to solve complex partial differential equations involve in multiphysics associated with flow over airfoil. It has better adaptive control over numerical uncertainty that can lead to errors in numerical results.

Comparison of C_p values for 0^o and 5.8^o degrees of angle of attack are shown in Figure 14. There are very little variations (less than 1% at x/c=0.4) among these two angles of attacks data. Variations are high (around 4% at x/c=0.3 and 0.9) and prominent for higher angle of attacks at the leading and trailing edge of airfoil. This leads conclusion that higher angle of attacks will have higher lift values hence performance of wind turbine.

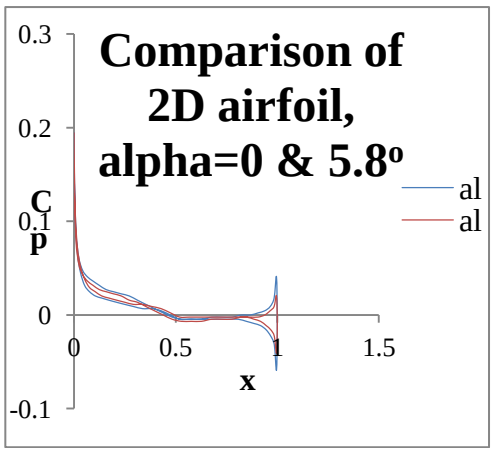

Fig 14. Comparison of *Cp* values for angle of attacks, $\alpha=0^o$ and 5.8^o.

5. CONCLUSIONS

CFD is used to predict the tapering and angles of attack that produce maximum power outputs for an untwisted horizontal axis wind turbine for 0 and 5.8^o angle of attack cases. By using the 2D drawing as the basis for design, the finding indicates that the tapering and angles of attacks have significant effects on wind turbine blade performance. Under typical design conditions tapering and angle of attacks were confirmed by the computation as significant design parameters. The presented results have helped the authors on the understanding of the flow physics around blade airfoil shapes. It has been followed that the definition to be used for comparison of the pressure coefficient using the stagnation pressure for the given shape, instead of the classical definition, since the first takes into account the influence of the local geometry. It has been shown that for attached flow conditions, the shape modifies the flow leading to 3D effects. CFD calculations can therefore be used to create simple airfoil to be implemented into 2D based methods that take into account a change in tapering and AOA. These shapes follow the current trend in the wind turbine industry, and resulted to be a good compromise. Further studies may be necessary to conceive an optimal blade shape, however this study served as a preliminary comparison to detect the main important parameters that may be taken into account for future designs.

ACKNOWLEDGMENTS

This study is based upon work supported by the NSF (National Science Foundation). The authors greatly acknowledge for the financial support of this work.

6. REFERENCES

1. Robert E. Wilson and Peter B.S. Lissman, NREL, Applied Aerodynamics of Wind Power Machines, 1974
2. Glauert H. Airplane Propellers. In Aerodynamic Theory, volume 4. Dover edition edition, 1963
3. Johansen J and Sørensen N.N. Numerical investigation of three wind turbine blade tips. Technical Report
4. Ferrer E and Munduate X. Cfd activities at cener. In IEA Annex XX symposium, Pamplona, Spain, May 2005.
5. Ferrer E and Munduate X. Wind turbine blade tip design using cfd. In Fluent user's meeting, Madrid, Spain, November 2006.
6. Ferrer E and Munduate X. Wind turbine blade tip comparison using CFD, Journal of Physics: Conference Series 75 (2007) 012005
7. Chalothorn Thumthae, Tawit Chitsomboon, Optimal angle of attack for untwisted blade wind turbine, Renewable Energy, Volume 34, Issue 5, May 2009, Pages 1279-1284,
8. Simulation Tutorial of FLUENT - Flow over an Airfoil- Problem Specification from: https://confluence.cornell.edu/display/SIMULATION/FLUENT+-+Flow+over+an+Airfoil-+Problem+Specification